CHAPTER I

INTRODUCTION

CHAPTER   1

INTRODUCTION

1.1   REVIEW   OF   InP

Research in semiconductor physics in the period
between 1940 and 1950 was primarily focussed on the ele-
mental semiconductors Germanium and Silicon. It was
Welker[1] who demonstrated in 1952 that the III-V compounds
are semiconductors with particularly interesting proper-
ties and that they have a close relationship with the
semiconducting elements of group - IV in the periodic
table. The spate of research that followed vastly exten-
ded the field of applications of III-V compound semiconduc-
tors. These developments also ushered in a new era of
materials research including new technologies for growth
and characterisation.

Indium Phosphide, a III-V semiconductor with
$E_g = 1.35$ at 300K, attracted immediate attention. Optical
absorption experiments by Oswald and Schade[2] in 1954
indicated the direct band-gap nature of the material.
Folberth and Weiss[3] reported the first detailed measurements
of electrical properties in 1955 and room temperature mobi-
lities of 4,500 cm^2/V.sec for $n = 6.3 \times 10^{15}$ cm^{-3} were

reported[4] as early as 1958. Laser action at 0.91 μm

in InP homojunctions was reported[5] within months of the

first reports on laser action in GaAs diodes. This ini-

tial enthusiasm did not last, due to the difficulties

encountered in preparing good quality single crystal

material.

Technological interest in Indium Phosphide was

revived in 1970 when Hilsum and Rees[6] suggested that its

band structure could be utilised to develop efficient

three-level transferred electron devices (TEDs). Although

these predictions have not been fully realised, they certa-

inly stimulated activity in the preparation of high quality

single crystals. The realisation in the mid 70s that InP

substrates due to lattice matching considerations are best

suited for fibre optic sources and detectors operating in

the low-loss wavelength region between 1.1 - 1.5 μm added

impetus to the increasing interest in this semiconductor.

Though similar in many respects with GaAs, inten-

sive investigations in the recent past have revealed that

Indium Phosphide has certain unique advantages over the

more widely known III-V semiconductors. It was shown,

for example, that the surface recombination velocity in

n-InP is 3 orders of magnitude less than GaAs[7], indicating

that higher luminescence efficiencies should be possible

with the former material. Walukiewicz et al[8] observed
that melt grown InP exhibited much lower compensation
than that encountered in melt grown GaAs. The higher
electron saturation velocity and higher threshold field
for avalanche break-down promise better high frequency
operation with higher power outputs and efficiencies
achievable as FETs and TEDs. Further the surface state
density has been shown to be much less compared with
GaAs, thus rendering InP a promising material for MIS
devices. Due to this combination of favourable electrical
and optical properties InP has emerged perhaps as the
third most important semiconductor after Si and GaAs.

Table 1.1 compares some of the material parameters
of InP and GaAs.

Table 1.1

Comparison of Material Parameters of InP and GaAs

Parameter	InP	GaAs
1	2	3
1. Structure	Zinc blende	Zinc blende
2. Band gap Eg. (eV) 300K	1.35 (Direct)	1.41 (Direct)
3. Lattice parameter($\overset{o}{A}$)	5.86875	5.65325
4. Density (gm/cc)	4.79	5.316

	1	2	3
5.	Coefficient of linear expansion ($^{\circ}C^{-1}$)	5.3×10^{-5}	6.63×10^{-5}
6.	Thermal conductivity ($W/Cm^{-\circ}C$)	0.68	0.44
7.	Refractive Index	3.450	3.655
8.	Static di-electric constant ($\varepsilon_s / \varepsilon_o$)	12.4	13.1
9.	High frequency dielectric constant ($\varepsilon / \varepsilon_o$)	9.55	10.91
10.	Electron affinity (eV)	4.4	4.05

Band Structure of Indium Phosphide -

The complete band structure of InP was determined
from electrc - reflectance measurements (EER) by Cardona
et al[9]. The results were consistent with the pseudo-
potential calculations of Cohen and Bergstresser.[10] The
major features of the energy band diagram are shown in
Fig.1.1. The conduction band consists of a lowest minimum
at the Γ point above which there are quadruply degenerate
L-minima in the (111) direction and triply degenerate
X-minima in the (100) direction respectively. The energy
differences $\Delta_{\Gamma L}$ and $\Delta_{\Gamma X}$ are 0.56 eV and 0.80 eV respec-
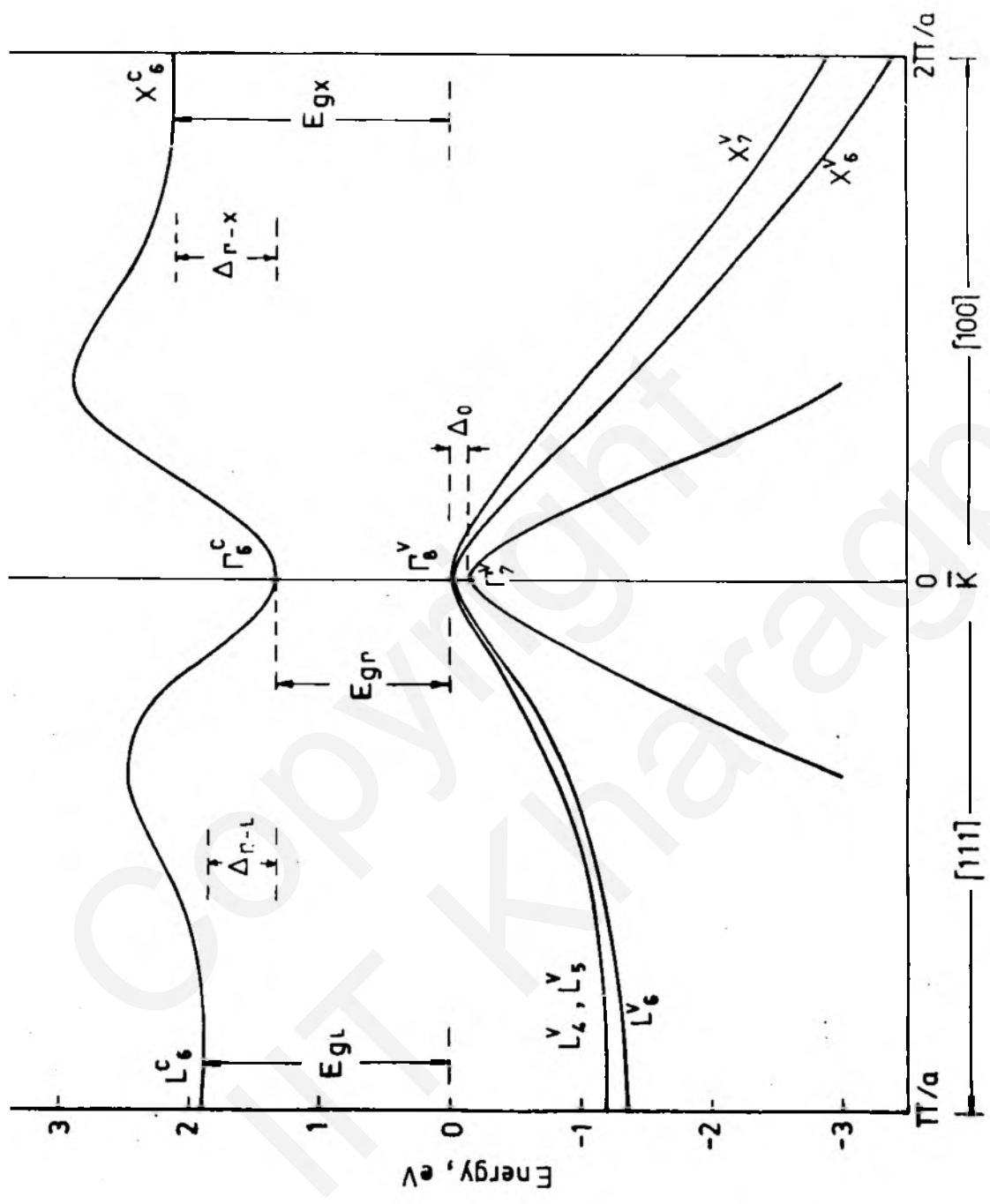tively at 300K. The valence band has three branches

Fig. 1.1 Band structure of InP.

Table 1.2 a

Conduction band parameters of Indium Phosphide

Band	Number of minima	Temperature dependence [*]			Pressure coefficient $(\partial E/\partial P)$ eV.K.bar^{-1}	Effective mass of electrons (m_c/m_o) [**]
		Eg(o)eV	α	β		
Γ	1	1.421	3.63×10^{-4}	162	9.5×10^{-3}	0.078
L	4	2.0	4.8×10^{-4}	162	3×10^{-3}	0.4
X	3	2.34	5.88×10^{-4}	162	1.5×10^{-3}	0.6

* The temperature dependence is expressed by Varshni equation

$$E_g(T) = E_g(o) - \frac{\alpha T^2}{(\beta+T)} \quad ; \quad T \text{ is expressed in } ^oK.$$

See Chapter 4 for details on temperature dependence of L and X bands.

** Density of states effective mass for one band.

Table 1.2 b

Valence band parameters of Indium Phosphide

Spin-orbit splitting $\Delta_o = 0.11$ eV

Heavy hole effective mass $(m_{hh}/m_o) = 0.56$

Light hole effective mass $(m_{lh}/m_o) = 0.12$

consisting of the heavy hole and light hole bands which
are degenerate at $\overline{K}=0$ and a third band 0.11 eV below the
others split off due to spin orbit interaction.

The temperature and pressure dependence of the
various energy gaps and the effective masses of conduction
electrons are shown in Table 1.2a. The valence band para-
meters are tabulated in Table 1.2b. The effective mass
of electrons in the Γ -minimum and those of heavy and
light holes have been obtained from cyclotron resonance
experiments.[11,12] Effective masses of electrons in the
L and X-bands have been deduced from the high pressure
work of Pitt[13] and from the high field transport properties
reported by Fawcett et al[14].
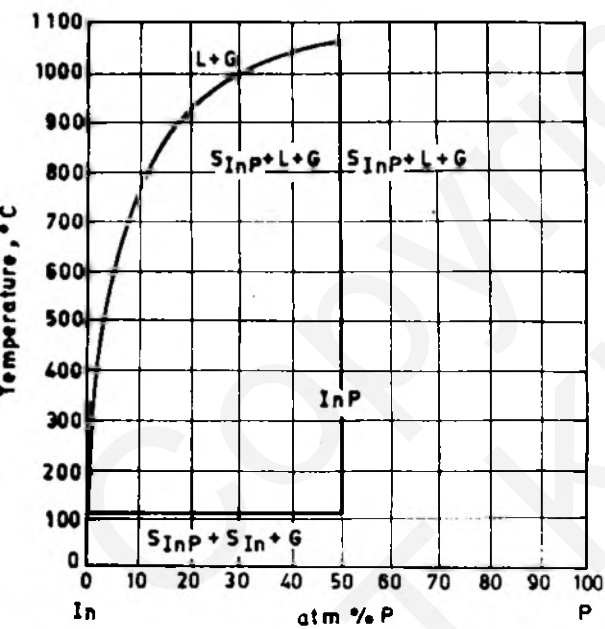
1.2   MATERIAL PREPARATION TECHNIQUES

(a)   Bulk Crystal Growth Methods -

The phase equilibria between solid compound melt
and vapor phases for InP[15] are shown in Fig.1.2. Important
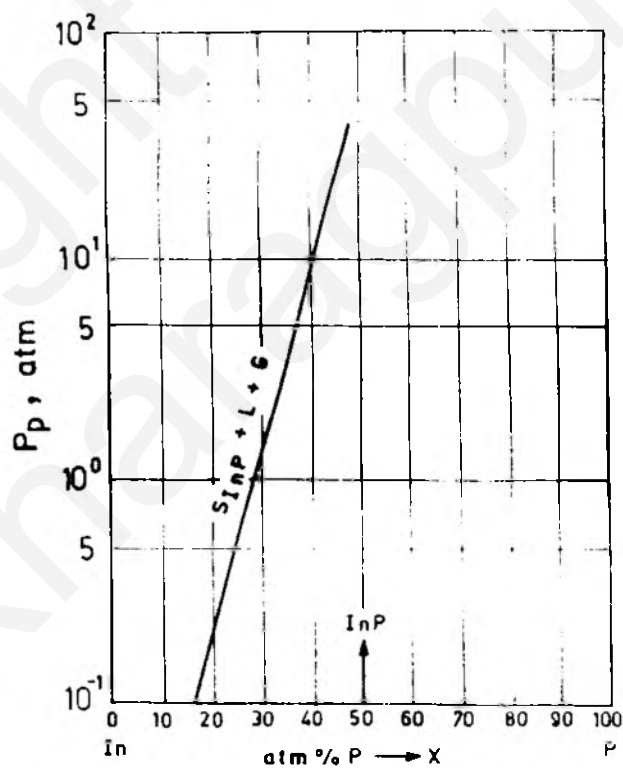data pertaining to growth are given in Table 1.3.
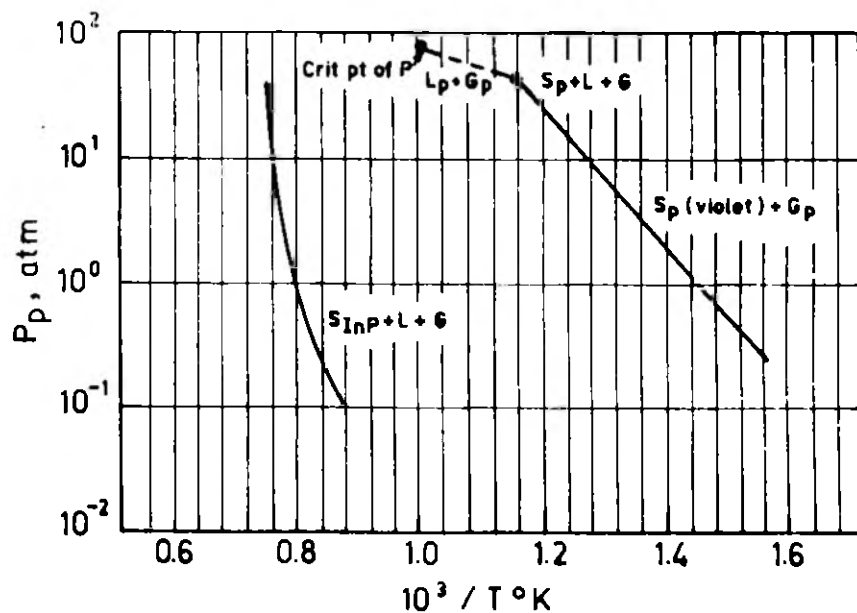
(a) P-T projection of the system InP.

b) T-x projection of the system InP.

(c) P-x projection of the system InP.

Fig. 1.2 Phase equilibria for the system InP.

Table 1.3

Thermodynamic Constants for InP

Temperature of Fusion T_F ($^{\circ}$K) 1335

Heat of Fusion H_F (KCal/g-atom) 6 ± 1.5

Entropy of fusion ΔS_F(Cal/mole $^{\circ}$K) 15.2

Interaction parameter $\alpha(T)$ $3578 - 3.54\ T$
  (Cal/mole)

Heat of atomisation (cohesive 153
  energy) ΔH (K Cal) at
  T = 910 $^{\circ}$K

Heat of reaction (K Cal) $InP(S) \longrightarrow In(l) + \frac{1}{2}\ P_2(g)$
  at T = 910°K
  $- \Delta H_T = 39.4$

  $InP(S) \longrightarrow In(l) + \frac{1}{4}\ P_4(g)$

  $- \Delta H_T = 27$

Bulk growth of Indium Phosphide starts with the synthesis of polycrystalline material, which is then used as the starting material for single crystal growth. The following methods are most commonly used for polycrystal growth - (i) horizontal Bridgman (ii) gradient freeze.

In the horizontal Bridgman technique sufficient quantities of elemental Indium and Phosphorous are kept at the two ends of an evacuated and sealed quartz tube. This tube is then placed in a two zone furnace such that the end containing Indium is at a temperature slightly higher than the melting temperature of the compound while the end containing Phosphorus is kept at about $600^{\circ}C$. The crystal is grown by moving either the furnace or the ampoule in such a way that the ampoule travels through a temperature gradient from the hot end to the cooler end. The vapor pressure of Phosphorus at the growth temperature is 27.5 atoms. Some of the problems encountered in conventional Bridgman growth have been overcome in a modified version known as high pressure Bridgman technique[16].

The gradient-freeze technique is similar to the horizontal Bridgman technique in that both produce crystalline material by gradual solidification of the melt. However, unlike Bridgman growth which requires the relative movement of the furnace and the crucible, in gradient-freeze

growth melt solidification takes place by the movement of a temperature gradient along the ingot. The chief advantage of this method lies in the fact that no relative movement between the furnace and the ampoule is required. On the other hand, the temperature required for crystal growth by this technique is higher because of the temperature gradient required above the melting point of the compound.

Single crystal growth is achieved usually by liquid encapsulated Czochralski technique (LEC). The polycrystalline material is contained in a Boron nitride crucible. To suppress the evaporation of phosphorus, the melt is covered by a liquid encapsulant which is often Borax (B_2O_3), and an inert gas over-pressure that exceeds the compound dissociation pressure is applied in the chamber. Single crystals are pulled by dipping a suitably oriented seed crystal through the encapsulant into the melt.

(b)   Epitaxial Growth   –

During bulk crystal growth, because of the large size of the crystal boule and the high temperature of growth, thermal stresses are created, as the crystal slowly emerges from the hot melt. These thermal stresses give rise to high dislocation densities in the crystal. Furthermore contamina-

tion with impurities from the melt container and specifically from the B_2O_3 encapsulant are unavoidable in this method. Thus bulk grown crystals have been found to be unfit for direct use in devices. It was realised that to obtain crystals with satisfactory structural perfection and accurately controlled impurity content; an additional growth process must complement these bulk growth methods.

Epitaxial growth satisfies the above requirements and provides single crystal layers suitable for device fabrication. Wafers sliced from bulk grown crystals are used as substrates for epitaxial growth. Epitaxial growth consists of deposition of thin crystalline films on lattice-matched substrates. When the deposited material has the same chemical composition as the substrate then the process is termed as homoepitaxy. On the other hand materials of chemical composition different from the substrate may also be grown provided the growing film has the same or related crystal structure and a lattice constant within 1 percent of the substrate. The process is then termed heteroepitaxy.

Currently two methods are widely used for the epitaxial growth of InP - Vapor phase epitaxy and Liquid phase epitaxy-depending upon whether the transport of the growing species occurs through vapor phase or through a

melt. Other epitaxial methods such as Molecular Beam
epitaxy (MBE) and Metalorganic chemical vapor deposition
(MOCVD) are also employed but are not discussed here.
Table 1.4 gives a comparison of VPE and LPE growth
technologies.

Table 1.4

Comparison between LPE and VPE

	Parameter	LPE	VPE
1.	Transport medium	liquid	vapor
2.	Growth temperature(typical)	$650^{o}C$	$700^{o}C$
3.	Growth rates (μm/hr)	1-100	5-50
4.	Typical rates(μm/hr)	10	10
4.	Structural quality	excellent	excellent
5.	Surface morphology	poor	good
6.	Thickness control	20 percent down to 0.1 μm	20 percent down to 0.1 μm
7.	Alloy compositional control	1 percent	5 percent
8.	Lowest carrier conc.(Cm^{-3})	10^{15}	10^{14}
9..	Dopant choice	wide	wide
10.	Undesirable effects* if any	none	deep levels present
11.	General	low cost easy to set up	costlier. Medium complexity.

* Ref.17

While LPE and VPE possess nearly comparable features LPE is more often used for opto-electronic devices because of the fact that in LEDs and lasers, highest luminescence efficiencies have been achieved by this method. Further it is easy to set up and maintain, unlike VPE in which very accurate control of gas flow and handling of hazardous gas mixtures requires complex and relatively expensive equipment. Because of the large selection of dopants which can be readily incorporated into the layers, LPE is especially useful when large doping concentrations are required.

The LPE process basically involves the deposition of material from a cooling solution onto an underlying substrate. The solution and substrate are kept apart in the growth apparatus initially and the solution is saturated with the growth material until the desired growth temperature is reached. The solution is then brought into contact with the substrate surface and allowed to cool at a rate and during a time interval which is appropriate for the desired layer. The driving force for nucleation is the supersaturation of the solution as the temperature is reduced. The crystals formed are those in which the free energy, which includes the surface energy, is minimised. Thus formation of an epitaxial layer is favoured when the lattice match is closest and/or the resultant change in the

shape of the crystal results in the smallest increase
in the surface energy.

Nelson[18] first reported the use of LPE for III-
V compound growth in 1963, using the "tipping technique".
Woodall and co-worker[19] later suggested a modified version
of LPE growth which is known as the "dipping technique".

Present day LPE apparatus, commonly make use of
"multibin sliding boat"[20] for LPE growth. A typical
multibin apparatus is shown schematically in Fig.1.3.
Layer growth takes place in a graphite boat which consists
of a moving slider "S", with recesses to hold the substrate
and a stationary graphite block 'B' provided with equi-
distant bins to hold the growth solution. Contact between
the growth solution and the substrate is achieved by moving
the slider. The main advantage of this system is that
several layers can be grown consecutively in a single growth
run, by successively pushing the substrate under different
bins. Growth is terminated by sliding the substrate away
from the growth solution. Care is taken to keep the gap
between the bottom surface of the slider and substrate very
small. Thus the sliding motion effectively wipes the melt
away from substrate surface at the end of growth.

To saturate the melt with the growth material it
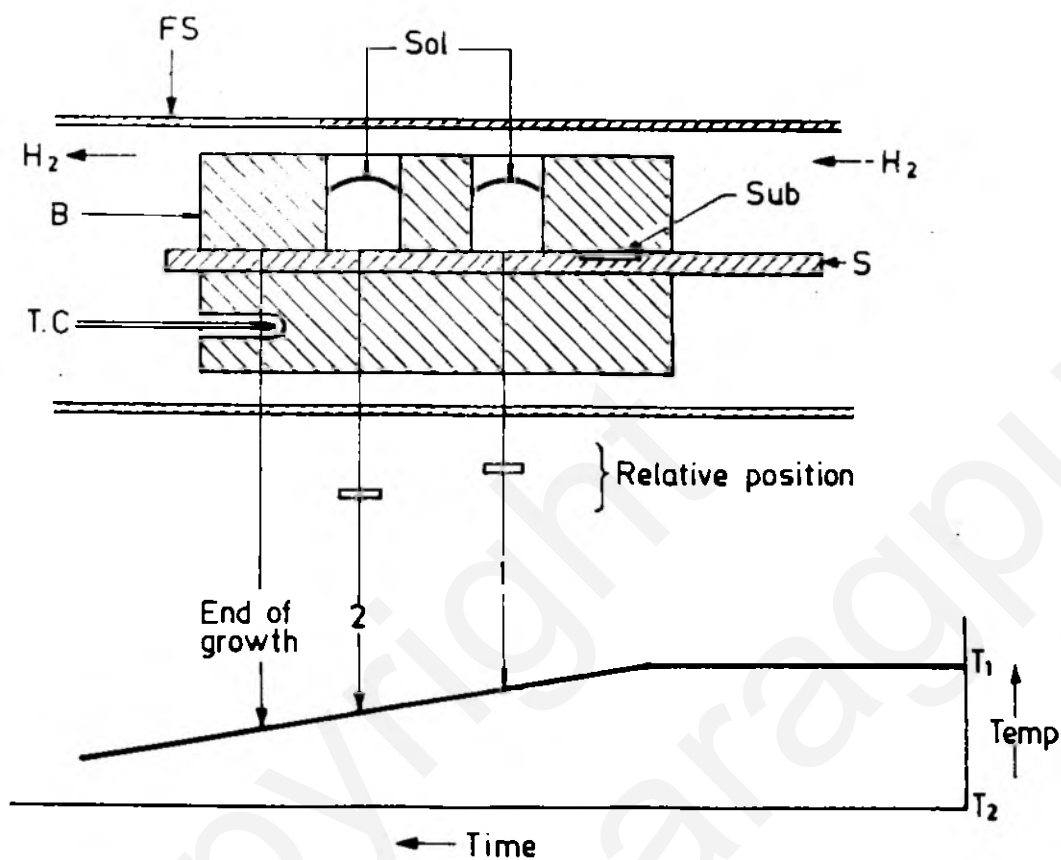
FS- FUSED SILICA FURNACE TUBE ; SOL - SOLUTIONS ; T.C- THERMOCOUPLE ; SUB - SUBSTRATE ;
S- SLIDER; B-BIN HOLDER.

Fig. 1.3 Schematic diagram of multibin apparatus.

is essential to know accurately the phase diagram for the
system at the growth temperature. Figure 1.4a gives the
liquidus curve for phosphorus in Indium for dilute solu-
tions[21] in the temperature range of interest for LPE
growth of InP. Figure 1.4b gives the dissociation press-
ure of phosphrus over InP in this temperature range. This
growth temperature is significantly less than the 750 -
850°C generally used for GaAs.

Doping in LPE is achieved by adding the impurities
directly to the melt. Incorporation of dopants into LPE
layers is conventionally defined in terms of the distribu-
tion coefficient, K_O, which represents the ratio of the
concentration of the impurity in the solid, C_s, to that
in the liquid C_L. Thus

$$K_O = \frac{C_s}{C_L} \qquad ..(1.1)$$

The group VI elements S, Se and Te act as donors
with low ionisation energy $[E_D \simeq 7-10\text{meV}]$ occupying
the P sites in InP while the group IIB elements Zn and Cd
and the group IIA elements Be and Mg act as acceptors
occupying the Indium sites. Unlike in GaAs, where Si and
Ge show amphoteric behaviour, all the group IV elements
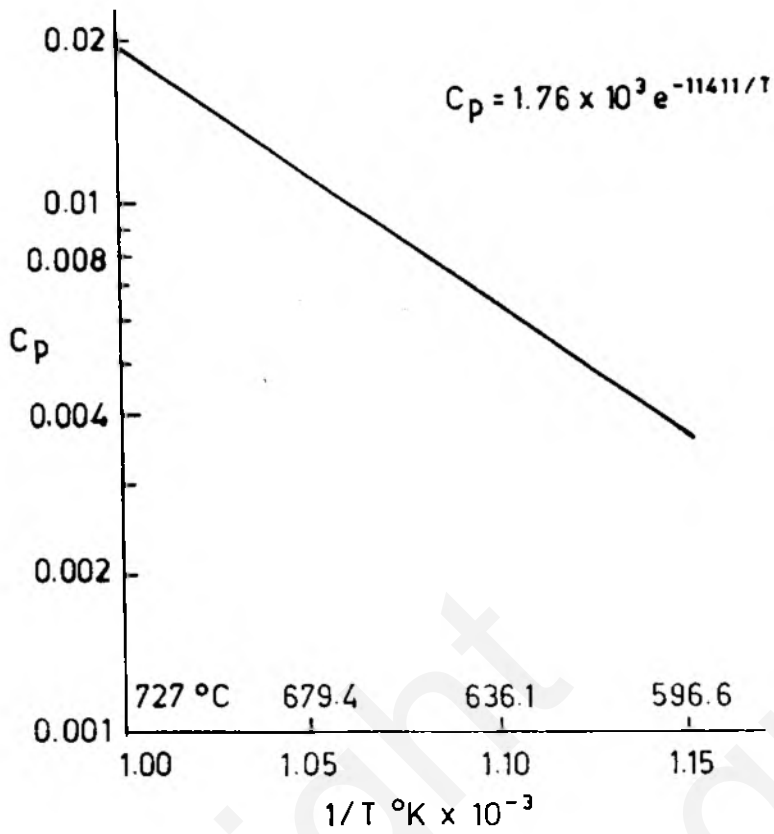behave as donors in InP. Relevant information for the

$$C_p = 1.76 \times 10^3 e^{-11411/T}$$

Fig. 1.4 (a) Mole fraction liquidus curve-P in In for dilute solutions.
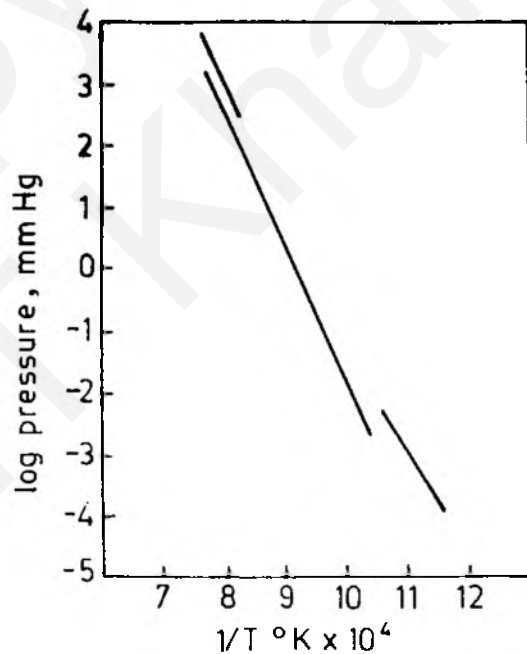
Fig. 1.4(b) Dissociation pressure of InP.

incorporation of impurities in LPE grown InP is tabulated in Tables 1.5 and 1.6.

Table 1.5

n-type Dopants in LPE of InP (Ref 22a and b)

Dopant	Distribution coefficient	Vapor pressure at $650^{\circ}C$ (Torr)	Covalent Tetrahedral atomic radius ($\overset{\circ}{A}$)
Si	30	10^{-10}	1.17
Ge	5×10^{-3}	10^{-10}	1.22
Sn	2×10^{-3}	3×10^{-9}	1.40
S	0.4 – 10	10^{3}	1.04
Se	4.2	500	1.14
Te	0.4	12	1.32

Table 1.6

P-type dopants in LPE of InP (Ref 22a and b)

Dopant	Distribution Coefficient	Ionisation energy(meV)	Vapor pressure at $650^{\circ}C$ (Torr)	Diffusion Coefficient (cm^2/Sec)	Covalent tetrahedral atomic radius ($\overset{\circ}{A}$)
Zn	0.7	47.3	2.5	3×10^{-11}	1.31
Cd	1×10^{-3}	56.3	200	3×10^{-12}	1.48
Mg	0.05 – 0.5	39.5	3	1×10^{-11}	1.40
Be	0.1	31	1×10^{-9}	–	1.06

An inspection of Table 1.5 indicates that for group IV elements the covalent radii increase in the order $\gamma_{Si} < \gamma_{Ge} < \gamma_{Sn}$. Since the smallest impurity is expected to substitute the easiest it can be seen that $K_{Si} > K_{Ge} > K_{Sn}$. Similar considerations also hold good in case of group VI elements.

The incorporation of group II elements appears more complex as can be seen from Table 1.6. Zinc is the most commonly used acceptor impurity in InP. Controlled doping with cadmium is difficult because of its high vapor pressure. On the other hand, because of its low diffusivity cadmium is preferred in cases where diffusion of the dopant during LPE growth should be minimised.

Experimental data showing the carrier concentration in LPE grown InP layers[23] as a function of the mole fraction of dopant in the growth solution is plotted in Fig.1.5. From the figure it can be seen that the carrier concentration in Zn-doped layers grown at $650^{o}C$ appears to saturate at about 3×10^{18} cm^{-3}.

1.3   BRIEF REVIEW OF HEAVILY DOPED SEMICONDUCTORS

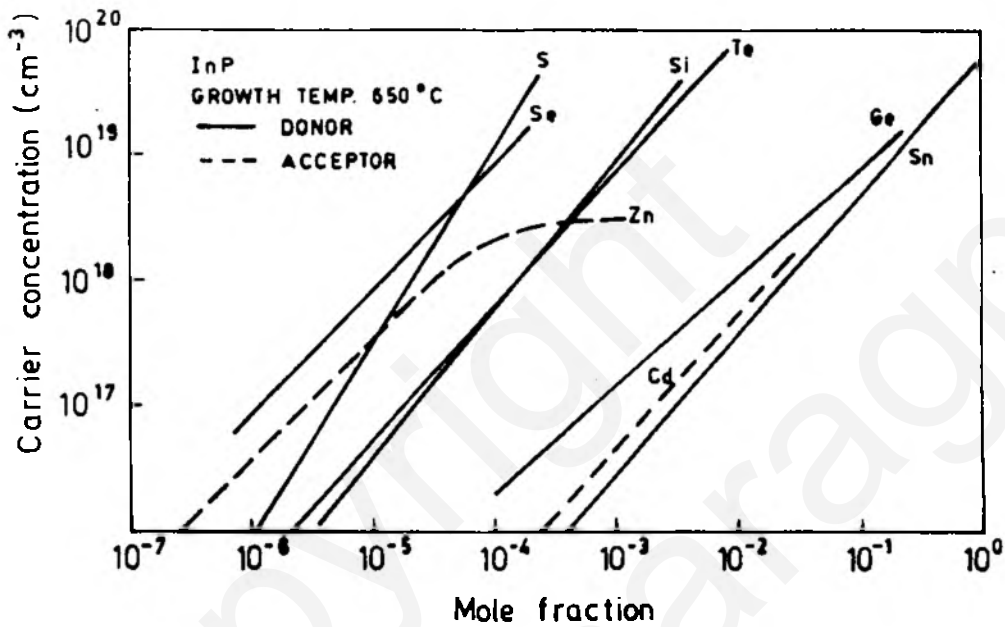When semiconductors are doped with small concentrations of donors or accepotrs these impurities from shallow

Fig. 1.5 Carrier concentration in InP LPE layers grown
at temperatures near 650°C as a function of
mole fraction of donor or acceptor impurity in
the growth solution.

energy levels close to the band edges. When the concentration of these impurities is increased the impurity ionisation energy gradually decreases due to the overlap of individual energy levels and the consequent formation of an impurity band. At some critical concentration n_c the ionisation energy becomes zero. Beyond this point the free carrier concentration (n) becomes independent of temperature. Semiconductors doped to this high level are known as heavily doped semiconductors. In quantitative terms a semiconductor is said to be heavily doped when the impurity content is greater than or equal to 1×10^{18} cm^{-3}.

The first interesting effect arising from heavy doping, was reported by Moss[24] and Burstein[25]. They observed that the optical absorption edge for n-type InSb varied significantly with the purity of the sample and moved to higher energies as the doping concentration was increased. They showed that because of the very light electron effective mass in InSb the conduction band states fill up rapidly as n is increased and the Fermi level moves above the bottom of the conduction band. This is known as the Moss-Burstein shift. Since the states below the Fermi level are all occupied, electronic transitions take place from the top of the valence band to states near or above the Fermi-level. It was also shown that this shift occurs to a much less extent in p-type material because of the

large effective mass of holes. Theoretical calculations based on Moss-Burstein shift alone, however, appeared to overestimate this shift in the absorption edge.

The development of Esaki diodes and laser diodes, which contain semiconducting layers doped upto 10^{19} cm^{-3} necessitated a clearer understanding of the effects of heavy doping. Thus it has been recognised that the random distribution of impurities at high concentrations distorts the band edges and changes the band edge effective mass. Theories have been developed, notably by Kane[26], Bonch-Bruevich[27] and Halperin and Lax[28], to describe the density of states near the band edge. Qualitatively all these theories predict the same result i.e., the random distribution of a large number of impurities produces potential fluctuations resulting in an asymmetrical tail of localised states below the band edge, and a rigid shift in the energy bands causing the so called band gap shrinkage. Free carrier screening effects were found to play an important role in determining the extent of band tailing and band gap shrinkage.

Band tailing effects were shown to be of negligible importance in determining the optical properties of heavily doped uncompensated semiconductors[29]. On the other hand band-gap shrinkage attracted much attention since it was

the combination of this parameter and the Fermi energy
that governed the shape of the optical absorption and
emission spectra. A number of theories have been proposed
and were reviewed by Abram et al[30] and Mahan[31]. A compari-
son of the experimental data on heavily doped semiconduc-
tors however shows major discrepancies between absorption
and photoluminescence as well as absorption and transport
measurements. It was pointed out by Wagner[32] that photo-
luminescence (PL) and photoluminescence excitation spectro-
scopy (PLE) techniques provide more reliable information
on band-gap shrinkage compared with optical absorption.
On the theoretical front there has been some disagreement[31]
over the use of Thomas-Fermi linear screening approximation
for the calculation of screening effects. There have also
been some differences between experimental and theoretical
results.[32]

Transport properties of heavily doped material
are governed mainly by the carrier-ionised impurity scatt-
ering even at room temperature. Electron mobility in
heavily doped semiconductors is often explained satisfacto-
rily using the Brooks-Herring theory[33] of impurity scatte-
ring, taking into consideration the effects of degeneracy.
However, for a closer fit it is felt that this theory
requires further refinements.

1.4   SCOPE AND MOTIVATION FOR THE THESIS

Recently there has been a considerable interest in
heavily doped Indium Phosphide. This interest is due
primarily to the expanding range of applications of this
material. Since both the effective band gap and the refra-
ctive index can be altered by heavy doping, such material
could be useful in optoelectronic devices for carrier or
photon confinement. Further it should be possible on
heavily doped material to achieve extremely low resistance
ohmic contacts, a major technological requirement.

Hawrylo[34] reported that LPE grown InP layers doped
with Se to $N_D - N_A$ 1×10^{20} cm^{-3} showed photoluminescence
at energies as high as 1.91 eV. Undoped InP on the other
hand shows a PL peak at 1.35 eV. This shift in the effective
band gap is much greater than that normally observed with
other heavily doped III-V semiconductors. Hawrylo also
observed that at these high doping levels of n $= 1 \times 10^{20}$,
the layers retained the crystal structure of InP with
a change of only -0.038 percent in the lattice parameter,
while exhibiting luminescence efficiencies in the visible
red region comparable to a number of ternary alloys such
as InGaP, and GaAsP.

Due to the above special features it should be

possible to make use of these layers for the fabrication
of useful devices. However, device fabrication calls for
a thorough understanding of the material and process
characteristics. Though carrier concentrations as high
as 1.7×10^{20} cm^{-3} had been achieved, very little further
work has been reported on heavily doped InP. Thus unlike
the case of GaAs, there has been a lack of systematic
study in correlating theory and experiment on the effects
of heavy doping in InP. These considerations formed the
principle motivation for the present work.

In this thesis an effort has been made to grow
heavily doped n-InP layers with carrier concentrations of
$n = 1 \times 10^{18}$ cm^{-3} to $n > 1 \times 10^{20}$ cm^{-3} and to study the
incorporation of the dopant at these high concentrations.
Liquid phase epitaxy was used to grow these layers with
Selenium as the dopant, since this would facilitate
unambiguous comparison of our results with those of
earlier workers[34,35]. Since it is essential for any
device application to have smooth surfaces and defect free
layers, we have studied the surface morphology and etch
pit densities with heavy doping in these layers. Mobility
and conductivity studies of the heavily doped layers have
been made in the temperature range 77 K - 300 K. An effort
has been made to explain these results on the basis of
established scaterring mechanisms in order to gain an insight

into the various physical processes that could be influencing the mobility. A theoretical model is proposed which includes the non-parabolicity of the Γ conduction band minimum and the effect of higher lying L bands, for the calculation of band tail parameters. On the basis of this model detailed computer calculations of screening length (L_S), Fermi level (E_F), band tail density of states and band gap shrinkage have been made for n-InP. Finally photoluminescence experiments were conducted to study the shift of the band-to-band emission to higher energies with heavy doping. These results were quantitatively explained using the results of computer calculations mentioned above.

The LPE growth procedure along with the instrumentation work under taken is described in Chapter 2. Growth rates and microprobe studies on the incorporation of Se at high doping levels are discussed first in Chapter 3. These are followed by surface morphology studies and etch pit measurements on Huber-etched samples. Chapter 4 contains the throretical model and the results of calculations of band tail parameters based on this model. Chapter 5 is divided into two parts - part A contains resistivity and Hall studies and part B contains photoluminescence studies. Finally in Chapter 6 the conclusions of the present investigation and suggestions for further work are presented.

REFERENCES

1. H.welker., Z.Naturforsch, 7a , 744 (1952).

2. F.Oswald and R.Schade., Z.Naturforsch, 9a, 611 (1954).

3. O.G.Folberth and K.Weiser., Z.Naturforsch, 10a, 615, (1955).

4. M.Glicksman and K.Weiser., J.Elec.Chem.Soc. 105, 728 (1958).

5. K.Weiser, R.S.Levitt, M.I.Nathan and G.Burns ., Solid. St. device conf., Lansing, Michigan, June 1963 (abstracts reported in IEEE Trans. Elec. devices ED-10, 334 (1963))

6. C.Hilsum and H.D.Rees., Electron. Lett, 6, 277 (1970).

7. H. C. Casey, Jr.,and E.Buehler, Appl. Phys. lett. 30 , 247 (1977).

8. W.Walukiewicz, J.Lagowski, L.Jastrzebski, P.Rava, M. Lichteusteiger, C.H.Gatos and H.C.Gatos, J. Appl. Phys, 51 , 2659 (1980).

9. M.Cardona, K.L.Shaklee and F.H.Pollak, Phys. Rev. 154, 696 (1967).

10. M.L.Cohen and T.K.Bergstresser, Phys. Rev. 141,789(1966)

11. L.Eaves, R.A.Stradling, S.Askenazy, J.Leotin, J.C.Portel and J.P.Ulmet, J.Phys.C Solid st.Phy. 4 , L42-47 (1971).

12. J.Leotin, R.Barbaste, S.Askenazy, M.S.Skolmik, R.A. Stradling and J.Tuchendler, Solid st.Comm. $\underline{15}$, 693, 1974

13. G.D.Pitt, J.Phy.C. Solid st.Phys, $\underline{6}$, 1586 (1973).

14. W.Fawcett and D.C.Herbert, J.Phys. C. Solid St.Phys. $\underline{7}$, 1641 (1974).

15. J.Vanden Boomgaard and K.Schol, Phillips Res rep $\underline{12}$, 127 - 140 (1957).

16. A.G.Fischer, J.Elec. Chem. Soc, $\underline{117}$, 41C (1970).

17. O.Wada, A.Majorfeld and A NMM Choudhury, J.Appl.Phys $\underline{51}$, 423 (1980)

18. H.Nelson RCA Rev $\underline{24}$, 603 (1963).

19. J.M.Woodall, H.Rupprecht and W.Reuter, J.E.Chem. soc. $\underline{116}$, 899, 1969

20. H.C.Casey. Jr. M.B.Panish, W.O.Schlosser and T.L. Paoli, J.Appl. Phys $\underline{45}$, 322 (1974).

21. J.J.Hsieh, Symp. on GaAs and related compounds, St. Louis (Inst. of Phys. London) p 74, 1976.

22.a) E.Kuphal, J.Crys. Growth, $\underline{54}$, 117 (1981) and references therein

   b) R.C.Evans, An Introduction to crystal chemistry, p 74, Cambridge University press, 1966.

23. J.J.Hsieh, Handbook on Semiconductors, p 415,
Ed. T.S.Moss, North Holland publishing
Co, New York (1980).

24. T.S.Moss, Proc.Phys. Soc. B, 67, 775, 1954.

25. E.Burstein, Phys. Rev, 93, 632 (1954).

26. E.O.Kane, Phys. Rev, 131, 79 (1963)

27. V.L.Bonch - Bruevich, "Semiconductors - Semimetals",
Eds R.K.Willardson and A.C.Beer, Vol 1,
p 101, Academic press, New York, 1966.

28. B.I.Halperin and M.Lax, Phys.Rev, 148, 722 (1966)

29. C.J.Hwang, J.Appl. Phys. 41, 2668 (1970); Phys. Rev.
B-2, 4117 (1970).

30. R.A.Abram, G.J.Rees and B.L.H.Wilson, Adv. in Phys.
27, 799 (1978)

31. G.D.Mahan, J.Appl. Phys, 51, 2634 (1980).

32. J.Wagner, Phys. Rev, 29, 2002 (1984).

33. R.B.Dingle, Phil.Mag, 46, 831 (1955).

34. F.Z.Hawrylo, Appl. Phys. Lett. 37, 1038 (1980).

35. P.M.Raccah, H. Rahemi and J.Zehnder,[*] Appl. Phys.
Lett., 39, 496 (1981).

* F.Z.Hawrylo and H.Kressel